

# Evaluation of Zeolite Acidity by $^{31}\text{P}$ MAS NMR Spectroscopy of Adsorbed Phosphine Oxides: Quantitative or Not?

Dmitry S. Zasukhin, Ivan A. Kasyanov, Yury G. Kolyagin, Anna I. Bulygina, Karl C. Kharas, and Irina I. Ivanova\*



Cite This: *ACS Omega* 2022, 7, 12318–12328



Read Online

ACCESS |



Metrics & More

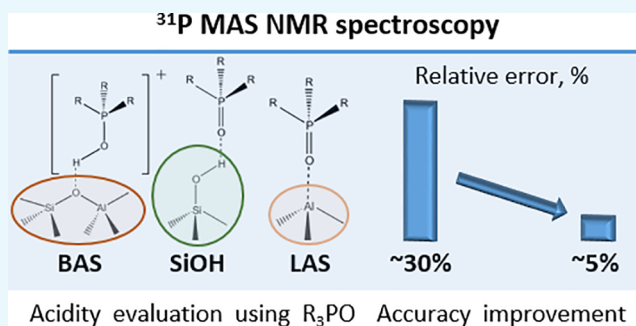


Article Recommendations



Supporting Information

**ABSTRACT:**  $^{31}\text{P}$  magic angle spinning nuclear magnetic resonance (MAS NMR) spectroscopy of adsorbed alkyl-substituted phosphine oxides has witnessed tremendous progress during the last years and has become one of the most informative and sensitive methods of zeolite acidity investigation. However, quantitative evaluation of the number of sites is still a challenge. This study clarifies the main origin of errors occurring during NMR experiments, introduces the appropriate standards (both internal and external), and determines the relaxation parameters and the conditions for the acquisition and integration of spectra. As a result, a methodology for the quantitative measurement of the content of Brønsted and Lewis sites and the amount of internal and external silanol groups is established. The application of probe molecules of different sizes (namely, trimethylphosphine oxide (TMPO), tri-*n*-butylphosphine oxide (TBPO), and tri-*n*-octylphosphine oxide (TOPO)) is shown to be a good tool for distinguishing between the active sites inside the zeolite pores, mesopores, and on the outer crystal surface. The methodology proposed is verified on BEA zeolites different in composition, texture, and morphology.



## 1. INTRODUCTION

Due to their unique textural and acidic properties, zeolites are widely used as solid catalysts in various heterogeneous catalytic processes.<sup>1</sup> The improvement of existing catalysts and the development of novel ones require detailed information on their acidity: type of acid sites (Brønsted (B)/Lewis (L)),<sup>2</sup> their concentration and strength, as well as their localization in zeolite material (inside the zeolitic porous system/in mesopores/on the outer surface of the crystal).

Many different analytical methods have been developed to characterize acid sites of zeolites.<sup>3,4</sup> The most widely used methods are thermoprogrammed desorption of ammonia (TPD- $\text{NH}_3$ ),<sup>5</sup> IR spectroscopy,<sup>6</sup> and  $^1\text{H}$  magic angle spinning nuclear magnetic resonance (MAS NMR) spectroscopy.<sup>7</sup> In addition, the adsorption of basic probe molecules studied by IR or MAS NMR spectroscopy is widely applied. Among the probe molecules, the most prevalent are pyridine (Py)<sup>6</sup> and its substituted homologues<sup>8</sup> in the case of IR spectroscopy and phosphorous-containing bases<sup>3</sup> in the case of MAS NMR spectroscopy. TPD- $\text{NH}_3$  provides useful information on the amount and strength of the acid sites, but it cannot determine their nature and localization. On the contrary, IR spectroscopy of adsorbed Py gives insight into the nature of sites (B/L) and their localization, but the quantitative evaluation is not always straightforward and could give underestimated results.<sup>9,10</sup>  $^{31}\text{P}$  MAS NMR of adsorbed P-containing bases is a promising

technique both for qualitative and quantitative evaluation of zeolite acidity.<sup>3,11,12</sup>

$^{31}\text{P}$  MAS NMR of adsorbed P-containing bases was first applied to investigate zeolites' acidity in the 1980s. Lunsford et al. studied the adsorption of trimethylphosphine (TMP) as a probe molecule to characterize the acidity of HY zeolite<sup>13</sup> and showed that the position of TMP signals in  $^{31}\text{P}$  MAS NMR spectrum could give information on the nature of sites and their strength. Since then,  $^{31}\text{P}$  NMR spectroscopy of adsorbed phosphines has received significant attention. Different phosphines, including trimethylphosphine, triethylphosphine,<sup>14</sup> tri-*n*-butylphosphine,<sup>14</sup> tricyclohexylphosphine,<sup>15</sup> and triphenylphosphine, were studied as probe molecules and applied to various solids, such as zeolites, heteropolyacids, and pure and modified metal oxides.<sup>11,12</sup> The results demonstrated that trialkylphosphines can be used to determine the number of B sites in zeolites but pointed out that they are not sensitive to the strength of B sites because of the narrow range of chemical shifts.<sup>13,16,17</sup> On the contrary, the signals correspond-

Received: February 9, 2022

Accepted: March 15, 2022

Published: March 29, 2022



ing to trialkylphosphine molecules adsorbed on L sites were observed in a wide spectral range.<sup>13,18–20</sup> This feature allowed to account for the strength of L sites using trialkylphosphines but resulted in overlapping with the signals of physically adsorbed trialkylphosphines, which prevented obtaining quantitative information. Another significant drawback of trialkylphosphines as probe molecules is their ability to oxidize during adsorption over zeolites.<sup>17,21</sup>

Lunsford and Zaleski et al.<sup>21</sup> showed that the application of trialkylphosphine oxides ( $R_3PO$ ) as probe molecules to characterize zeolite acidity has several advantages to trialkylphosphines. First, these probe molecules are stable and do not oxidize over zeolites during sample preparation. Second, they are more sensitive to the nature and strength of Brønsted acid sites compared to phosphine molecules.<sup>22</sup> Osegovic and Drago<sup>23</sup> found that chemical shift correlates with the heat of adsorption onto the acid site. Later, Zheng et al.<sup>22</sup> found a linear correlation between the chemical shifts of protonated  $R_3PO$  homologues and the proton affinity. Finally, the application of trialkylphosphine oxides is very perspective for the investigation of L sites in zeotypes with different heteroatoms, such as Sn, Zr, and Ti.<sup>25</sup> However, it should be mentioned that they are less applicable for the investigation of L sites in Al-containing zeolites because of overlapping of signals for B and L sites.

Among  $R_3PO$ , trimethyl,<sup>16,24,26,27</sup> tri-*n*-butyl,<sup>22,24</sup> tri-*n*-octyl,<sup>22</sup> and triphenyl<sup>28</sup> phosphine oxides are most often used as probe molecules. By variation of the length of *n*-alkyl chains, it is possible to determine the localization of acid sites on the internal/external surface of zeolites in micro-/mesopores and distinguish sites with different accessibility.<sup>11</sup> These probe molecules can mimic substrates in catalytic reactions.<sup>3</sup>

Thus, the literature data show that  $^{31}P$  MAS NMR spectroscopy of adsorbed alkyl-substituted phosphine oxides has witnessed tremendous progress during the last years and has become one of the most informative and sensitive methods of zeolite acidity investigation. However, quantitative evaluation of acid sites is still a big issue for this method.<sup>12</sup> The main problems are related to both the methodology of sample preparation for NMR measurements and the conditions of NMR spectra registration.

In this study, we aimed to clarify the main origin of errors occurring during samples preparation and NMR experiments, to choose the appropriate standards (both internal and external), to determine the relaxation parameters and the conditions for the acquisition of spectra, and to develop the methodology for quantitative measurement of the number of acid sites by  $^{31}P$  MAS NMR spectroscopy of adsorbed phosphine oxides. To verify this methodology, BEA zeolites with different amounts of Brønsted and Lewis acid sites as well as internal and external silanol groups were used.

## 2. EXPERIMENTAL SECTION

**2.1. Zeolite Materials.** Zeolite materials studied involved commercially available samples of BEA zeolites CP811C and CP814Q with Si/Al = 150 and 25 (hereinafter Al-BEA-150 and Al-BEA-25, respectively) from Zeolyst, as well as synthesized siliceous zeolite BEA (Si-BEA) and dealuminated zeolite BEA (DeAl-BEA). Physicochemical characteristics of the samples are presented in Figures S1–S3.

Si-BEA sample was synthesized by conventional fluoride synthesis according to the following procedure:<sup>29</sup> 30.13 g of

tetraethyl orthosilicate (TEOS) and 33.88 g of 35% aqueous tetraethylammonium hydroxide solution (TEAOH) were mixed in a plastic beaker. The mixture was stirred on a magnetic stirrer until evaporation to a weight of 36.75 g. Then, 3.26 g of HF solution in water (48 wt %) was added to the resulting mixture and thoroughly homogenized. The resulting reaction mixture with the composition  $SiO_2/0.54$  TEAOH/ $0.54$  HF/ $5.6$   $H_2O$  was placed in a Teflon autoclave and left for crystallization for 10 days at 140 °C. The obtained samples were washed on a Buchner funnel with 4 L of distilled water and then dried at 60 °C.

The DeAl-BEA sample was prepared by dealumination of a commercially available Zeolyst CP814C zeolite. For this, 10 g of BEA zeolite sample was mixed in a glass conical flask with 300 mL of concentrated nitric acid. The flask with the reaction mixture was placed on a magnetic stirrer, a reflux condenser was connected, the temperature was increased to 90 °C and left under stirring for about 14 h. Then, the sample was washed in a centrifuge until the filtrate pH was 6–7 and left to dry at a temperature of 60 °C. This procedure was repeated three times to ensure the completeness of the dealumination process.

**2.2. Probe Molecules.** Trialkylphosphine oxide ( $R_3PO$ ) probe molecules, namely, trimethylphosphine oxide (TMPO), tri-*n*-butylphosphine oxide (TBPO), and tri-*n*-octylphosphine oxide (TOPO), were supplied by Merck.

**2.3. Reference Compounds for Internal and External Standards.** Reference compounds for standards including calcium, diammonium, and monopotassium phosphates, as well as gallium phosphide, were also supplied by Merck.

Aluminum phosphate with a tridymite structure ( $AlPO_4$ -tridymite) was synthesized according to the following procedure:<sup>30</sup> 7.49 g of aluminum nitrate nonahydrate ( $Al(NO_3)_3 \times 9H_2O$ ) and 2.64 g of diammonium phosphate ( $(NH_4)_2HPO_4$ ) were dissolved in 200 mL of distilled water in a glass beaker with a volume of 250 mL. Then, after 15 min of stirring the mixture on a magnetic stirrer, 2 mL of concentrated nitric acid was added. The mixture was left under stirring on a magnetic stirrer for another 15 min, after which the reaction mixture was left to dry at a temperature of 90 °C for a couple of hours. After complete drying, the resulting precipitate was washed with water in a centrifuge and left at 60 °C for drying. After second drying, the obtained samples were calcined in a furnace for 6 h at 850 °C.

Silicoaluminophosphate SAPO-34 was prepared by the hydrothermal synthesis in an autoclave, rotated at a speed of 5 rpm, from the reaction mixture of  $Al_2O_3/2$   $P_2O_5/0.6$   $SiO_2/4$  TEAOH/ $70$   $H_2O$  molar composition for 25 h at 190 °C.<sup>31</sup> The reactants were aluminum isopropoxide, silica sol (40 wt %), phosphoric acid (85 wt %), and tetraethylammonium hydroxide (35% aqueous solution). After crystallization, the product was separated from the liquid phase by centrifugation, washed, dried at 70 °C for 12 h, and calcined at 600 °C for 6 h in a dry-air stream.

**2.4. Characterization Techniques.** The chemical composition of the samples was determined by X-ray fluorescence analysis on a Thermo Scientific ARL Perform'X instrument equipped with a 3.5 kW rhodium tube. X-ray diffraction (XRD) patterns were recorded on a Bruker D2 PHASER diffractometer (Cu  $K\alpha$  radiation) in an angular range of  $5^\circ < 2\theta < 50^\circ$ . The diffraction patterns were processed using the Bruker DIFFRAC.EVA software package. Phases were identified according to the ICDD PDF2 database. Electron microscope images of the samples were recorded on a JEOL

JEM 2010 transmission electron microscope using a 200 keV electron beam. Sorption/desorption isotherms of nitrogen were measured at 77 K using an automated porosimeter (Micromeritics ASAP 2020). Micropore volumes ( $V_{\text{micro}}$ ) were determined using the  $t$ -plot method. The total sorbed volumes ( $V_{\text{tot}}$ ), including adsorption in the micropores and mesopores and on the external surface, were calculated from the amount of nitrogen adsorbed at relative pressure  $p/p_0$  of 0.95 before the onset of interparticle condensation.

Fourier transform infrared (FTIR) spectra were recorded on a Nicolet Protégé 460 FTIR spectrometer equipped with an MCT detector with an optical resolution of  $4\text{ cm}^{-1}$  in a range of  $4000\text{--}400\text{ cm}^{-1}$ . Before the measurements, the zeolites were pressed into self-supported pellets and activated in the infrared (IR) cell attached to a vacuum line at 673 K for 1 h. Adsorption of pyridine was performed at 423 K for 30 min. The probe molecules excess was further evacuated at 423 K for 15 min. The amounts of Brønsted and Lewis acid sites were determined from the intensities of the bands at ca. 1546 and  $1455\text{ cm}^{-1}$  of adsorbed pyridine, respectively, using the molar extinction coefficients from the literature.<sup>32</sup>

**2.5. MAS NMR Spectroscopy.** The solid-state  $^{31}\text{P}$  NMR spectra were recorded on a BRUKER AVANCE-II NMR 400 WB spectrometer with a magnetic field of 9.4 T. Samples were packed into a 4 mm diameter zirconia rotor under dry-air conditions and spun at the magic angle in 4 mm H/X MAS WVT probe at 10.5 kHz. The direct polarization (DP) and Hahn-echo (HE) pulse sequences combined with preliminary signal saturation and high-power proton decoupling during the acquisition were used in this study.<sup>31</sup>  $90^\circ$  pulse was equal to 2.1  $\mu\text{s}$ . Recycle delay was varied from 20 to 3600 s. The swept-frequency two-pulse phase modulation (SW-TPPM) sequence ( $\tau = 8\text{ }\mu\text{s}$ ,  $\varphi = 15^\circ$ ) was used for proton decoupling.<sup>33</sup>  $T_1$  relaxation times were measured by saturation-recovery pseudo-two-dimensional (2D) experiments<sup>34</sup> with echo detection to prevent the baseline distortions. Concentrated phosphoric acid was used as a chemical shift reference (0 ppm).

### 3. RESULTS AND DISCUSSION

**3.1. Origin of Errors Occurring during Quantification of  $^{31}\text{P}$  MAS NMR Data.** Since trialkylphosphine oxides are solid compounds, the general procedure of sample preparation for  $^{31}\text{P}$  MAS NMR measurements involves the dissolution of the selected trialkylphosphine oxide in appropriate solvent and impregnation of zeolite sample with an appropriate amount of solution. In some cases, loading of probe molecule can be accomplished without solvent<sup>28</sup> by thoroughly mixing corresponding trialkylphosphine oxide with zeolite sample. In this case, the subsequent heating of the mixture at an elevated temperature<sup>35</sup> is required for the diffusion of the probe molecule to the active sites. The most commonly used solvent for the impregnation procedure is dichloromethane ( $\text{CH}_2\text{Cl}_2$ );<sup>28,36</sup> however other solvents such as tetrahydrofuran<sup>14</sup> are also reported. The impregnation with the solution of probe molecules is followed by solvent removal, which is usually accomplished by heating the sample on the vacuum line at  $50\text{--}80\text{ }^\circ\text{C}$ .<sup>25,36</sup> To ensure uniform adsorption of probe molecules, after evacuation, the samples are usually subjected to thermal treatment at  $165\text{--}200\text{ }^\circ\text{C}$ <sup>37</sup> or ultrasonication.<sup>28</sup> This procedure seems to be the most favorable as low partial pressures of solid  $\text{R}_3\text{PO}$  probe molecules do not allow adsorption onto the zeolite surface from the gaseous phase.

To assess the cause of possible errors accumulated during sample preparation, which may affect the further quantitative assessment of the NMR data, we used the most common deposition technique described.<sup>12,36</sup> According to this procedure, a weighed portion of the sample is placed into a glass ampoule and connected to a vacuum line. The sample is heated up to  $400\text{ }^\circ\text{C}$  for 7 h and maintained at this temperature for another 7 h to remove water and other possible impurities. A solution of the selected probe molecule (TMPO, TBPO, or TOPO) in dichloromethane ( $\text{CH}_2\text{Cl}_2$ ) is prepared in a glass jar. The concentration is adjusted to achieve the proper content of the probe molecule in the sample, taking into account the known volume of the injected solution (80  $\mu\text{L}$ ). Afterward, this portion of solution is added to the sample in a dry glovebox using a microsyringe, and the ampoule is again connected to the vacuum line to remove the solvent. After complete removal of the solvent (until a pressure of  $1 \times 10^{-5}$  Torr was reached), the ampoule with the sample is sealed off and heated for 2 h at  $200\text{ }^\circ\text{C}$ . Finally, the ampoule is opened in a dry glovebox and the sample is transferred into an NMR rotor for further measurements. The typical NMR spectra of various probe molecules adsorbed on Al-BEA-25 using a single-pulse sequence with proton decoupling are shown in Figure 1. The  $^{31}\text{P}$  MAS NMR spectra of bulk TMPO, TBPO, and TOPO are presented in Figure S4.

The spectrum of TMPO adsorbed over Al-BEA-25 shows very broad signals, complicating its analysis and integration. The broadening of signals can be associated either with the

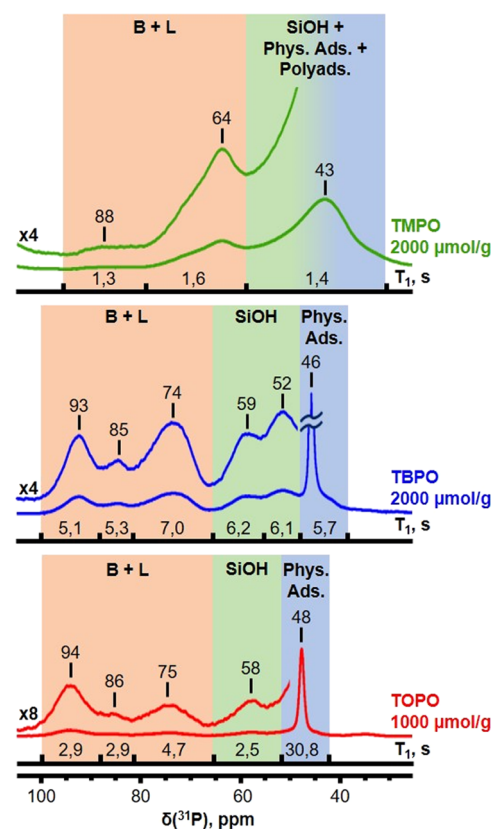


**Figure 1.**  $^{31}\text{P}$  DP MAS NMR spectra of adsorbed  $\text{R}_3\text{PO}$  on Al-BEA-25 zeolite (number of scans in the sample spectrum (NS) = 1024; recycle delay times (RDT) = 20 s). The amount of adsorbed  $\text{R}_3\text{PO}$  is given in  $\mu\text{mol/g}$ .  $T_1$  relaxation times measured for each signal are shown below the spectra.



self-adsorption of probe molecules or their interaction with water.<sup>27</sup> The signals of TMPO are shifted to the lower field to the TBPO and TOPO.<sup>11</sup> The lines in the 64–88 ppm range are due to TMPO adsorbed on acidic B + L sites, whereas the broad signal at ca. 43 ppm contains overlapping signals of physisorbed TMPO, TMPO adsorbed on silanol groups, as well as a signal of TMPO polyadsorption on Brønsted acid sites.<sup>38</sup>

The spectra of TBPO and TOPO contain well-resolved NMR lines with similar positions. According to the literature data,<sup>3,24,39</sup> the narrow line in the range of 46–48 ppm can be attributed to physically adsorbed R<sub>3</sub>PO, whereas the signals in the range of 74–94 ppm are due to acidic B and L sites with different strengths. For the Al-BEA-25 sample, these lines should be mostly due to B sites, but the presence of L sites cannot be excluded. As mentioned already, the signals of B and L sites can overlap in the spectra of phosphine oxides adsorbed over zeolites.<sup>22,26</sup> The lines in the 52–59 ppm region were assigned to the adsorption of R<sub>3</sub>PO on silanol groups as will be further discussed in Section 3.7.

In an attempt to obtain quantitative data, we performed several experiments over Al-BEA-25 under different experimental conditions. The variable parameters involved R<sub>3</sub>PO loadings and recycle delay times (RDT). The same set of experiments were performed for various probe molecules, including TMPO, TBPO, and TOPO. The results are presented in Table S1. The content of different sites presented in Table S1 was calculated from the relative intensities of the signals.<sup>16</sup> The regions of spectra corresponding to R<sub>3</sub>PO adsorption on different sites and physisorbed R<sub>3</sub>PO were integrated, and the overall integral intensity of the spectrum was normalized to the number of adsorbed probe molecules, yielding the content of probe molecules adsorbed on various sites ( $C_i$ ,  $\mu\text{mol/g}$ )

$$C_i = \frac{n_i}{m_{\text{zeol}}} = \frac{I_i}{I_{\text{total}}} \times \frac{n_{\text{total}}}{m_{\text{zeol}}} \quad (1)$$

where  $n_i$  is the number of probe molecules adsorbed on  $i$ -th region ( $\mu\text{mol}$ );  $m_{\text{zeol}}$  is the mass of zeolite in MAS rotor (g);  $I_i$  is the integral intensity of  $i$ -th region;  $I_{\text{total}}$  is the integral intensity of the whole spectrum; and  $n_{\text{total}}$  is the total number of adsorbed probe molecules ( $\mu\text{mol}$ ).

This approach assumes that all probe molecules introduced in the sample are observed in the NMR spectrum, and it does not take into account the possible loss of probe molecules during the sample preparation. The analysis of the results presented in Table S1 reveals that the calculated number of acid sites depends on both probe loadings and RDTs. The increase of loadings leads to lower values of acid sites determined, which points to a systematic error. This error is most probably related to the higher loss of the excess probe molecules on the ampoule walls at higher loadings, whereas lower loadings lead to complete consumption of probe molecules in the porous system of zeolite sample. The variation of RDTs does not show specific trends.

The statistical analysis of the data (Table 1) shows significant deviations from the average values. The relative error for different probe molecules is within 26–33%, which is rather high for quantitative assessment of acidity. The average acidity measured by TMPO and TBPO is similar and close to the theoretical amount of Al in the sample but does not correspond to the total acidity measured by FTIR spectroscopy

**Table 1. Preliminary Assessment of the Acidity of Al-BEA-25 Zeolite**

probe molecules	total acidity ( $\mu\text{mol/g}$ )	relative error (%)	total acidity by IRS of adsorbed Py ( $\mu\text{mol/g}$ )	theoretical amount of Al in zeolite ( $\mu\text{mol/g}$ )
TMPO	620 $\pm$ 160	26	425	600
TBPO	600 $\pm$ 170	28		
TOPO	240 $\pm$ 80	33		

of adsorbed Py. The acidity measured by TOPO is much lower than the values obtained with other probe molecules, pointing out that only part of acid sites is accessible for TOPO.

The analysis of the reasons for high errors observed during NMR data quantification led us to the conclusion that there are three main sources of errors: (i) loss of probe molecules during preparation procedure; (ii) incomplete relaxation of <sup>31</sup>P nuclei; and (iii) incorrect integration of NMR spectra.

The loss of probe molecules during sample preparation can arise from the use of volatile dichloromethane as a solvent, which can lead to a change in the concentration of the probe solution, from the adsorption of probe molecules on the walls of the ampoule and from other minor errors that inevitably accumulate in the course of the preparation process before recording the spectra. To accurately determine the number of probe molecules loaded onto the sample, one should use external or internal standards. However, there are only a few works in which external or internal standards were applied.<sup>16,37</sup> In these studies, diammonium hydrophosphate (NH<sub>4</sub>)<sub>2</sub>HPO<sub>4</sub> was used as a reference compound for external and internal standards. A detailed search for the optimal reference compounds has not been performed so far.

Incomplete relaxation of <sup>31</sup>P nuclei could be related to low RDT values. To obtain quantitative data, RDT values should be 3–5 times higher than spin-lattice relaxation times ( $T_1$ ).<sup>27</sup> Otherwise, the signal intensity will be underestimated owing to the lack of complete relaxation. Therefore, the accurate measurement of spin-lattice relaxation times is required for all individual and adsorbed probe molecules as well as for the reference compounds.

Finally, incorrect integration of spectra can arise from the following problems. Since phosphorus nuclei have strong anisotropy, a big part of the signal intensity (up to one-third of the total intensity) can be in spinning side bands (SSB). Therefore, it is necessary to integrate not only the central signal, but also all SSB. At the same time, due to the presence of a time delay between the excitation pulse and the beginning of the free induction decay (FID) registration (pre-scan delay), the first points in the FID are “cut off”. This, in turn, leads to distortion of the baseline and the need to correct it for the integration of all SSB (Figure S5). This procedure depends on the way of execution and leads to significant errors.

Therefore, for quantitative measurement of acidity by <sup>31</sup>P MAS NMR spectroscopy of adsorbed phosphine oxides, it is necessary to select the appropriate standards (both internal and external), to determine the relaxation parameters and the conditions for the acquisition of spectra and to develop the procedure for quantitative integration of <sup>31</sup>P MAS NMR spectra.

### 3.2. Selection of External and Internal Standards.

Table 2 summarizes the main requirements for external and internal standards for <sup>31</sup>P MAS NMR studies of adsorbed probe molecules. First of all, both internal and external standards should be chemically stable, pure, and have the exact

Table 2. Requirements for Solid External and Internal Standards

compounds	general requirements for both internal and external standards		requirements for an internal standard		
	exact composition and high purity	chemical stability	suitable chemical shift	no interaction with probe molecules or zeolite	low specific surface area, no competitive adsorption
inorganic (ionic) phosphates	+/-	+/-	-	+	+
AlPO and SAPO materials	+	+	+	+	+/-
metal phosphides	+	+/-	+	+/-	+

composition. Besides, there are additional requirements for the internal standards: (i) it should have a suitable chemical shift so that its signals do not overlap either with the signals of the adsorbed probe molecules or with their SSB; (ii) it should not interact with probe molecules or with the zeolite samples; and (iii) it should have a low specific surface area to avoid excessive physical adsorption of the probe molecules.

To meet these requirements, we considered three groups of compounds: ionic phosphates ( $(\text{NH}_4)_2\text{HPO}_4$ ,  $\text{KH}_2\text{PO}_4$ ,  $\text{Ca}_3(\text{PO}_4)_2$ ), covalent phosphates ( $\text{AlPO}_4$ -tridymite and SAPO-34), and metal phosphides (GaP). The results of their analysis are presented in Figure 2 and Table 3.

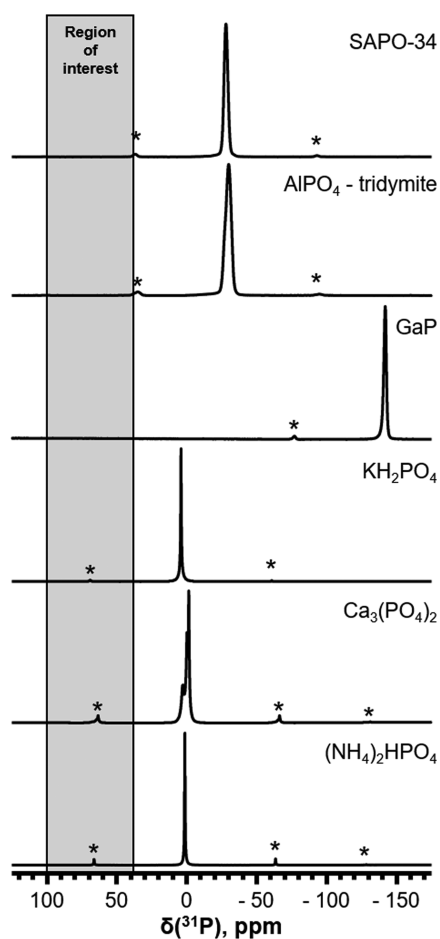


Figure 2.  $^{31}\text{P}$  DP MAS NMR spectra of reference materials for internal and external standard (NS = 32; RDT(SAPO-34) = 120 s, RDT( $\text{AlPO}_4$ -tridymite) = 3600 s, RDT (GaP) = 120 s, RDT( $\text{KH}_2\text{PO}_4$ ) = 1200 s, RDT( $\text{Ca}_3(\text{PO}_4)_2$ ) = 40 s, RDT( $(\text{NH}_4)_2\text{HPO}_4$ ) = 60 s). \* denote spinning side bands.

Table 3.  $T_1$  Values for Individual Probe Molecules and Reference Compounds

substance	$T_1$ (s)
TMPO	4
TBPO	6
TOPO	300
$(\text{NH}_4)_2\text{HPO}_4$	10
$\text{KH}_2\text{PO}_4$	200
$\text{Ca}_3(\text{PO}_4)_2$	5
$\text{AlPO}_4$ -tridymite	450
GaP	20
SAPO-34	20

Figure 2 shows the  $^{31}\text{P}$  MAS NMR spectra of selected reference compounds. The region of interest corresponding to the signals of probe molecules adsorbed on acid sites is marked with gray color. Since this region is rather broad, the rotation frequency should be high enough to avoid overlapping the SSB of the internal standard with the signals of probe molecules. In our case (9.4 T magnet), the rotation speed was 10.5 kHz.

The spectrum of calcium phosphate shows several broad asymmetrical signals, which arise from phase impurities (e.g., calcium hydrophosphate  $\text{CaHPO}_4$ , calcium dihydrophosphate  $\text{Ca}(\text{H}_2\text{PO}_4)_2$ , etc.), which prevents it from being used as a standard. The other two metal phosphates ( $(\text{NH}_4)_2\text{HPO}_4$  and  $\text{KH}_2\text{PO}_4$ ) show narrow NMR signals and can be applied as external standards. However, none of the metal phosphates can be used as an internal standard since their SSB overlaps with the region of interest and can interfere with integrating the signals of probe molecules and the quantitative evaluation of acid sites. Besides, ammonium salts of phosphoric acid are unstable and start to decompose even during mechanical grinding;  $(\text{NH}_4)_2\text{HPO}_4$  easily converts into monoammonium phosphate according to the equation  $(\text{NH}_4)_2\text{HPO}_4 \rightarrow \text{NH}_4\text{H}_2\text{PO}_4 + \text{NH}_3\uparrow$ .

GaP shows a narrow signal at ca.  $-141$  ppm. The main signal and its SSB do not overlap with the region of interest. However, this material might decompose upon grinding in mortar during mixing with zeolite and therefore cannot be used as an internal standard.

Covalent phosphates  $\text{AlPO}_4$ -tridymite and SAPO-34 show the only NMR lines with suitable chemical shifts. SAPO-34 has a high surface area, well-developed porous structure, and acid sites, and therefore, it cannot be used as an internal standard, whereas  $\text{AlPO}_4$ -tridymite meets all of the requirements for internal standards. Its only drawback is the long relaxation time ( $T_1 = 450$  s). Therefore, applying  $\text{AlPO}_4$  tridymite as an internal standard requires adapting specific spectra registration procedures.

**3.3. Determination of Spin-Lattice Relaxation Times.** It is known<sup>40</sup> that to obtain quantitative data from NMR

spectra recorded using a simple single-pulse sequence, it is necessary to ensure the complete relaxation of nuclei. As mentioned earlier, the time delay between two consecutive scans (RDT) must be at least 3–5 times longer than  $T_1$ . To meet this requirement, we measured spin-lattice relaxation times and determined minimum RDTs for all individual and adsorbed probe molecules, as well as for the reference compounds. For  $T_1$  measurement, we used the well-known procedure.<sup>27</sup> In the case of adsorbed probe molecules, we had to estimate the average spin-relaxation times for the defined regions. The results are presented in Table 3 and Figure 1. More details and raw data are provided in the Supporting Information (Figure S6).

The results presented in Table 3 show that all of the individual compounds except TOPO,  $\text{KH}_2\text{PO}_4$ , and  $\text{AlPO}_4$ -tridymite have rather short relaxation times. The same result relates to the adsorbed TMPO, TBPO, and TOPO probe molecules on BEA zeolite. In this case,  $T_1$  values were found to be within 1–7 s (Figure 1). Only in the case of physically adsorbed TOPO species,  $T_1$  values were higher than 30 s, which, on the one hand, does not interfere with the evaluation of acid sites, but, on the other hand, limits the possibility of getting correct values for the total amount of TOPO adsorbed.

Thus, the results suggest that for quantitative measurements of adsorbed probe molecules, an RDT of about 40 s is enough, but to obtain quantitative data for internal standard ( $\text{AlPO}_4$ -tridymite) selected in this work, a long RDT is needed. There are several approaches reported in the literature, which allow one to reduce the time required for recording this kind of spectra, such as registration of spectra using small (“Ernst”) angle pulse.<sup>41</sup> However, this method is susceptible to the parameters of the spectra registration. Therefore, we measured two independent spectra for the experiments with  $\text{AlPO}_4$ -tridymite as an internal standard. The first one—with a short RDT (40 s) and a large number of scans—was to ensure a good signal-to-noise ratio, whereas, the second spectrum—with a low number of scans and a long RDT (3600 s)—was to ensure complete relaxation of phosphorus nuclei of  $\text{AlPO}_4$ -tridymite and physisorbed TOPO.

**3.4. Integration of Spectra.** Another important source of errors mentioned earlier is the baseline distortions observed in single-pulse experiments (Figure S5a), which makes it difficult to integrate SSB correctly. To solve this problem, we record the spectra with a Hahn-echo (HE) pulse sequence (Figure S5b). Due to the peculiarities of such spectra, no baseline distortion is observed in them. Although these spectra are not quantitative, the ratio of intensities of the central line and SSB is the same as in single-pulse experiments. The accurate integration of the central peak and the SSB allows us to determine the constant  $k^{\text{CSA}}$  (CSA—chemical shift anisotropy)

$$k^{\text{CSA}} = \frac{I_{\text{total}}(\text{HE})}{I^{\text{cl}}(\text{HE})} \quad (2)$$

where  $I_{\text{total}}$  is the total signal intensity (the sum of the integrals of the central line and SSB) in the Hahn-echo spectrum and  $I^{\text{cl}}$  is the intensity of the central signal in Hahn-echo spectrum.

Multiplying the intensity of the central line signal from the single-pulse experiment by this constant allows us to take into account the intensity of SSB. This approach was used for quantitative spectra integration.

**3.5. Application of Quantitative Approach for Zeolite Al-BEA-25 Acidity Characterization.** Considering three

main sources of errors (loss of probe molecules during preparation procedure; incomplete relaxation of  $^{31}\text{P}$  nuclei; incorrect integration of NMR spectra), two procedures were elaborated for the quantitative estimation of the content of acid sites by  $^{31}\text{P}$  MAS NMR of adsorbed probe molecules.

The first procedure was based on applying the external standard, appropriate RDTs, and  $k^{\text{CSA}}$  correction factor. In this case, the  $^{31}\text{P}$  MAS NMR spectra of the sample and the reference were recorded separately. The RDT value of 40 s was applied for the sample, whereas for the external standard, the RDT value was selected to ensure complete relaxation of phosphorus nuclei of the standard according to Table 3. Using this procedure, the number of probe molecules adsorbed on the  $i$ -th site was calculated from the ratio of corrected and normalized intensities of the  $i$ -th line in the spectrum of the sample and the reference line in the spectrum of the external standard, this ratio being multiplied by the known amount of  $^{31}\text{P}$  nuclei taken in the reference sample. To obtain the content of sites, the number of probe molecules adsorbed on  $i$ -th sites was normalized to zeolite mass. Taking that, the overall formula for the calculation of the content of  $i$ -th sites was as follows

$$C_i = \frac{n_i}{m_{\text{zeol}}} = \frac{I_i^{\text{cl}} \times (k_i^{\text{CSA}}/\text{NS})}{I_{\text{std}}^{\text{cl}} \times (k_{\text{std}}^{\text{CSA}}/\text{NS}_{\text{std}})} \times \frac{n_{\text{std}}}{m_{\text{zeol}}} \quad (3)$$

where  $n_i$  is the number of probe molecules adsorbed on  $i$ -th sites ( $\mu\text{mol}$ );  $m_{\text{zeol}}$  is the mass of zeolite in MAS rotor (g);  $I_i^{\text{cl}}$  is the integral intensity of the central line in  $i$ -th region of the spectrum under study;  $I_{\text{std}}^{\text{cl}}$  is the integral intensity of the central line in the spectrum of standard material;  $k^{\text{CSA}}$  is the correction factor associated with the intensity of SSB signals; NS is the number of scans in the sample spectrum;  $\text{NS}_{\text{std}}$  is the number of scans in the spectrum of standard material; and  $n_{\text{std}}$  is the number of  $^{31}\text{P}$  nuclei in the reference sample ( $\mu\text{mol}$ ).

The second procedure differs from the described above by applying an internal standard. In this case, the sample and the reference were thoroughly mixed in one pot and placed into the NMR rotor. However, because of the high  $T_1$  value measured for  $\text{AlPO}_4$ -tridymite internal standard, we acquired individual spectra for the sample and the reference as was discussed above. The calculation procedure was the same as in the case of the external reference.<sup>3</sup>

The main advantage of the first method was its simplicity from the point of view of sample preparation. However, the second procedure was more accurate since it provided the identical conditions of NMR spectra registration for the sample and reference.

Some valuable points should be mentioned with respect to eq 3. First, the result calculated by eq 3 does not depend on the absolute values of the integral signal intensities of the sample and the standard but on their ratio— $I_i^{\text{cl}}/I_{\text{std}}^{\text{cl}}$ . Therefore, the calculation of concentrations using this equation is not affected by the inhomogeneous radio frequency excitation/detection profile over the sample in the MAS NMR rotor, which is present in every solid-state NMR probe. To obtain a reliable result, it is important that the sample and the standard substance distributions inside a MAS rotor are similar. In the case of the external standard, the location of the sample in the MAS rotor should be controlled and application of the Teflon spacers<sup>42</sup> would be useful. In the case of the internal standard, the homogeneous mixing of the standard with the sample is important. Another point is that for the internal standard, the



**Table 4. Quantitative Assessment of the Acidity of Al-BEA-25 by  $^{31}\text{P}$  MAS NMR of Adsorbed TBPO (2000  $\mu\text{mol/g}$ ) Using Various Standards**

experiment	standard	B + L ( $\mu\text{mol/g}$ )	SiOH ( $\mu\text{mol/g}$ )	phys. ads. ( $\mu\text{mol/g}$ )	total amount adsorbed ( $\mu\text{mol/g}$ )
without standard		625	505	870	2000 <sup>a</sup>
with external standard	( $\text{NH}_4$ ) <sub>2</sub> HPO <sub>4</sub>	395	400	495	1290
	AlPO <sub>4</sub> -tridymite	395	400	495	1290
	GaP	395	400	495	1290
	KH <sub>2</sub> PO <sub>4</sub>	510	520	645	1675
	SAPO-34	510	520	640	1670
	pure TBPO	430	435	540	1405
with internal standard	AlPO <sub>4</sub> -tridymite	405	360	610	1365

<sup>a</sup>Without taking into account the loss of probe molecules during sample preparation.

ratio  $n_{\text{std}}/m_{\text{zeol}}$  can be calculated more precisely since it is set experimentally during the sample preparation and does not depend on sample packing in the MAS rotor. When using the external standard, accurate measurements of the standard and the sample packed masses are required, which is an additional source of errors.

Table 4 shows the results of a quantitative assessment of the  $^{31}\text{P}$  MAS NMR spectra of TBPO adsorbed on zeolite Al-BEA-25 using various standards. First of all, the application of standards reveals that the total number of probe molecules adsorbed on the sample is much less than those taken for the adsorption owing to significant losses during sample preparation. This significantly decreases the values for acidic sites and silanol groups with respect to the values obtained without a standard. On the other hand, the comparison of the data obtained with various standards shows that in the case of ( $\text{NH}_4$ )<sub>2</sub>HPO<sub>4</sub>, GaP, and AlPO<sub>4</sub>-tridymite external standards, the results are very close to those revealed by the internal standard. On the contrary, the application of KH<sub>2</sub>PO<sub>4</sub>, SAPO-34, and pure TBPO shows significant deviations. This observation can be explained by changing the *Q*-factor of the NMR probe, and therefore its absolute sensitivity, when recording the spectra of samples of different nature.<sup>43,44</sup> The rotor with the sample being inside the detection coil acts as a core. By putting various materials into the rotor, we change the magnetic properties of the coil and, as a result, change the *Q*-factor of the oscillatory circuit. Moreover, the obtained results were influenced not only by the magnetic properties of the substance itself but also by all of the impurities in it, especially water.

Thus, although using an external standard is simpler, it does not always lead to accurate results, and the application of internal standards seems to be more reliable.

**3.6. Zeolite Al-BEA-25 Acidity Characterization.** Applying this methodology, we repeated the experiments on the adsorption of various probe molecules over Al-BEA-25 using AlPO<sub>4</sub>-tridymite as an internal standard and Hahn-echo pulse sequence to take into account the contribution of SSB. The results are presented in Tables 5 and S2.

**Table 5. Quantitative Assessment of the Acidity of Zeolite Al-BEA-25**

probe molecules	total acidity ( $\mu\text{mol/g}$ )	relative error (%)	total acidity by IRS of adsorbed Py ( $\mu\text{mol/g}$ )	theoretical amount of Al in zeolite ( $\mu\text{mol/g}$ )
TMPO	550 ± 20	4	425	600
TBPO	405 ± 15	4		
TOPO	160 ± 10	6		

The data analysis shows that the relative error decreased to 4–6%, and the main errors are associated with baseline and phase correction procedures. The data obtained became more reasonable compared to FTIR Py and the content of Al in the zeolite

- TMPO probe molecule has the smallest size. It can easily enter the pores of BEA zeolite and can interact with all its acidic sites. The number of sites measured by TMPO corresponds to the content of Al in the sample. But overdose of probe molecules in the sample can lead to overlapping of signals in  $^{31}\text{P}$  MAS NMR spectra, resulting in incorrect determination of acid sites content and preventing distinguishing of the peaks corresponding to silanol groups. Therefore, the amount of TMPO adsorbed should be close to the number of acid sites in the studied sample.
- The number of sites measured by TBPO coincides with the data obtained by FTIR Py. Most probably, TBPO can enter the pores of zeolite BEA, but it cannot measure all of the sites owing to sterical hindrances. In particular, it cannot measure the sites located close to each other.
- TOPO molecule has the biggest size and, most probably, cannot enter the pores of zeolite BEA. It measures the sites at the outer surface of the crystals and in the pore mouths. The results show that almost half of the zeolite acid sites are located close to the external surface of the crystal.

Thus, the application of three probe molecules with different sizes allows distinguishing the acid sites with different localization.

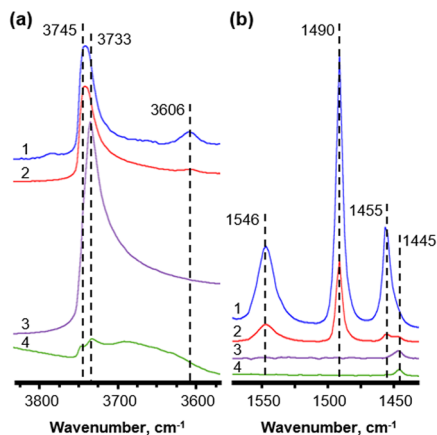
**3.7. Application of the Quantitative Approach to Zeolites BEA with Different Compositions.** For the evaluation of acidity, we selected four samples of zeolite BEA with different compositions: two commercial zeolites with different Si/Al ratios (Al-BEA-25 and Al-BEA-150), strongly dealuminated zeolite (DeAl-BEA), and purely silicious, low-defect Si-BEA were synthesized by the fluoride route. The main characteristics of zeolite samples are presented in Table 6 and Figures S1–S3.

Zeolites Al-BEA-25, Al-BEA-150, and DeAl-BEA have similar textural characteristics and crystal sizes within 0.2–1  $\mu\text{m}$  (Table 6). Sample Si-BEA consists of the biggest crystals of 2–5  $\mu\text{m}$  (Figure S3) due to the application of the fluoride route of synthesis.

The acidity of the samples was characterized by FTIR spectroscopy in the region of OH group vibration and the region of adsorbed Py (Figure 3). In the OH region, three

**Table 6. Characteristics of BEA Samples**

sample	Si/Al molar ratio	$V_{\text{tot}}$ (cm <sup>3</sup> /g)	$V_{\text{micro}}$ (cm <sup>3</sup> /g)	crystal size ( $\mu\text{m}$ )
Si-BEA	$\infty$	0.24	0.16	2.0–5.4
DeAl-BEA	640	0.29	0.18	0.2–0.9
Al-BEA-150	135	0.24	0.18	0.1–1.1
Al-BEA-25	27	0.34	0.22	0.3–1.0

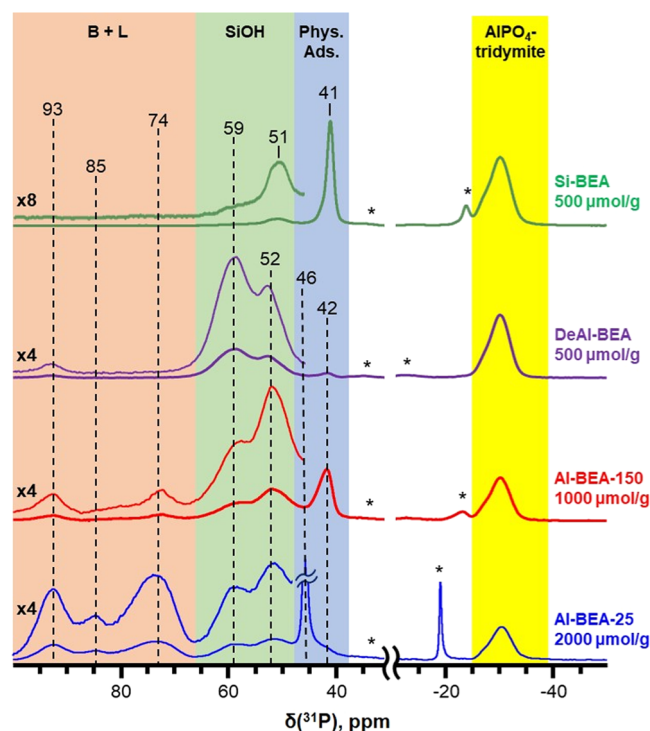
**Figure 3.** FTIR spectra in the region of OH group vibration (a) and in the region of adsorbed Py (b) on different BEA materials: (1) Al-BEA-25, (2) Al-BEA-150, (3) DeAl-BEA, (4) Si-BEA

characteristic bands are observed. The bands at 3745 and 3733 cm<sup>-1</sup> correspond to the external and internal silanol groups,<sup>45</sup> whereas the band at 3606 cm<sup>-1</sup> is due to the bridging hydroxyl groups (Si-(OH)-Al).<sup>46</sup> The latter is observed only in the case of Al-BEA-25 and Al-BEA-150. In the FTIR spectra of adsorbed Py (Figure 3b), the oscillation region of the spectra shows four characteristic bands. The band at 1546 cm<sup>-1</sup> corresponds to the interaction of Py with B sites, and the band at 1455 cm<sup>-1</sup> is due to Py adsorbed on L sites.<sup>47</sup> The band at 1490 cm<sup>-1</sup> is attributed to both PyH<sup>+</sup> and coordinately bound pyridine, whereas the band at 1445 cm<sup>-1</sup> can be assigned to pyridine interacting with SiOH groups.<sup>32</sup> The quantitative assessment of the data is presented in Table 7.

The results presented in Figure 3 and Table 7 show that the highest number of acidic B + L sites is observed in Al-BEA-25, with the highest Al content. The decrease of Al content (Al-BEA-150) leads to the proportional decrease of the total number of acidic sites and the increase of the contribution of B sites with respect to L sites. The sample after dealumination also shows trace amounts of B and L sites, which appear as a low-intensity broad band at 1546 cm<sup>-1</sup> and a shoulder at 1455 cm<sup>-1</sup>, respectively. The band at 1445 cm<sup>-1</sup> in the spectra of DeAl-BEA after Py adsorption and the intensive band at 3733 cm<sup>-1</sup> in the region of OH group vibration suggest that the

dealumination procedure leads to the formation of silanol defects, represented mainly by internal silanol groups. Sample Si-BEA shows only the lines corresponding to SiOH groups.

Figure 4 shows the <sup>31</sup>P MAS NMR spectra of adsorbed TBPO over BEA materials. The most intensive signals in the

**Figure 4.** <sup>31</sup>P MAS NMR spectra of TBPO adsorbed on different BEA materials with AlPO<sub>4</sub>-tridymite as internal standard (NS = 512; RDT = 40 s). \* denotes spinning sidebands. The amount of adsorbed TBPO is given in  $\mu\text{mol/g}$ .

range of 70–100 ppm corresponding to TBPO adsorbed over to B and L sites are observed in the case of the Al-BEA-25 sample, which has the highest Al content. Sample Al-BEA-150 shows similar lines in this region but with lower intensity. In the case of DeAl-BEA, the only line at ca. 93 ppm with low intensity is observed. The spectrum for the Si-BEA sample does not show any signals in the range of B and L sites, but it contains two small signals in the range of 51–59 ppm, which can be assigned to TBPO adsorbed over SiOH groups. Since the Si-BEA sample was synthesized in a fluoride medium, the contribution of internal silanols should be negligible over this sample. Consequently, more intensive signal at ca. 51 ppm was assigned to the external silanol groups, whereas a shoulder at ca. 59 ppm—to the internal silanols. The intensity of both signals at ca. 52 and 59 ppm increased significantly in the spectra of Al-containing and dealuminated BEA samples. This

**Table 7. Quantitative Assessment of Acidity of BEA Samples by <sup>31</sup>P MAS NMR of Adsorbed TBPO and FTIR of Adsorbed Py**

sample	<sup>31</sup> P MAS NMR, $\mu\text{mol/g}$			FTIR Py, $\mu\text{mol/g}$		N(Al), $\mu\text{mol/g}$
	B + L	SiOH, internal	SiOH, external	BAS	LAS	
Si-BEA	0 <sup>a</sup>	20 ± 1	65 ± 3	0	0	0
DeAl-BEA	30 ± 1	300 ± 12	190 ± 8	25	5	30
Al-BEA-150	120 ± 5	175 ± 7	275 ± 11	60	10	120
Al-BEA-25	405 ± 15	155 ± 6	215 ± 9	280	145	600

<sup>a</sup>Negligible amount.



is related to the formation of internal defects in the alkaline medium and the decrease of the crystal size (Table 5, Figure S3), leading to the increase of the outer surface, rich in external silanols.<sup>48</sup> For the DeAl-BEA sample, the intensity of the signal at 59 ppm increases compared to the signal at 53 ppm, due to the formation of internal silanol groups during the dealumination procedure. All of these observations are in line with FTIR data in the region of OH group vibration (Figure 3a).

The quantitative assessment of the acid sites content obtained from <sup>31</sup>P MAS NMR spectra of TBPO adsorbed on different BEA samples is shown in Table 7. The results are compared with the data obtained by FTIR spectroscopy of adsorbed Py and elemental analysis. For the sample with a high Al content (Al-BEA-25), the results obtained by <sup>31</sup>P MAS NMR and FTIR are in good agreement and show lower values than expected from chemical analysis. This observation could be due to the too short distance between the neighboring acid sites, which interfere with the adsorption of two probe molecules. In the case of Al-BEA-150 and DeAl-BEA with a lower Al content, the number of acid sites determined by <sup>31</sup>P MAS NMR corresponds to elemental analysis, whereas FTIR data remain to be underestimated. Sample Si-BEA shows only silanol groups, which can be also quantified by <sup>31</sup>P MAS NMR of adsorbed TBPO. The highest amount of silanol groups is observed over DeAl-BEA, which has the highest number of defects generated by the dealumination procedure, whereas the lowest amount of silanols is found over the hydrophobic Si-BEA sample. It is also important to note that the high content of SiOH groups determined by <sup>31</sup>P MAS NMR of adsorbed TBPO in the case of BEA samples obtained in alkaline media is in line with <sup>1</sup>H MAS NMR spectra (Figure S7).

In general, the acidity values obtained by IR spectroscopy of adsorbed pyridine are lower than the aluminum content in the zeolites and the values obtained by the <sup>31</sup>P MAS NMR spectroscopy of adsorbed TBPO. This may indicate a greater sensitivity of the NMR spectroscopy of adsorbed trialkylphosphine oxides for the quantitative analysis of acid sites. Moreover, <sup>31</sup>P MAS NMR of adsorbed trialkylphosphine oxides can be used for the quantitative analysis of both external and internal silanol groups, which cannot be assessed by other methods.

#### 4. CONCLUSIONS

The analysis of the reasons for rather high errors observed during the determination of zeolite acidity by <sup>31</sup>P MAS NMR spectroscopy of adsorbed alkyl-substituted phosphine oxides leads to the conclusion that there are three main sources of errors: (i) loss of probe molecules during the preparation procedure; (ii) incomplete relaxation of <sup>31</sup>P nuclei; and (iii) incorrect integration of NMR spectra. To ensure quantitative results, different external and internal standards for <sup>31</sup>P MAS NMR measurements were examined, the relaxation parameters and the conditions for the acquisition of spectra were determined, and the procedure for quantitative integration of <sup>31</sup>P MAS NMR spectra was developed.

Among the different external and internal standards investigated, (NH<sub>4</sub>)<sub>2</sub>HPO<sub>4</sub>, GaP, and AlPO<sub>4</sub>-tridymite are proposed as external standards, whereas AlPO<sub>4</sub>-tridymite is selected as the internal standard for NMR spectroscopic measurements. Although the use of an external standard is found to be simpler, the application of an internal standard is concluded to be more reliable.

The accurate measurement of spin-lattice relaxation times for all individual and adsorbed TMPO, TBPO, and TOPO probe molecules, as well as for the reference compounds, suggests that for quantitative measurements of adsorbed probe molecules, relatively short RDTs (40 s) are required, but to obtain quantitative data for AlPO<sub>4</sub> tridymite internal standard, a long RDT of 3600 s is needed.

It is proposed that the problems with baseline distortion observed in single-pulse experiments and leading to incorrect integration of SSB can be solved by recording the spectra with a Hahn-echo pulse sequence and the determination of correction factor, which takes into account the intensity contribution of SSB.

Considering different sources of errors, the methodology for quantitative measurement of the content of B and L acid sites by <sup>31</sup>P MAS NMR of adsorbed probe molecules is established. Moreover, it is demonstrated that <sup>31</sup>P MAS NMR of adsorbed trialkylphosphine oxides can be used for the quantitative analysis of silanol groups, both external and internal, which cannot be assessed by other methods.

The proposed methodology is verified on zeolites BEA with different compositions, textures, and morphologies. The application of probe molecules of different sizes (namely, TMPO, TBPO, and TOPO) is shown to be a good tool for distinguishing between the active sites inside the zeolite pores, mesopores, and on the outer crystal surface.

#### ■ ASSOCIATED CONTENT

##### SI Supporting Information

The Supporting Information is available free of charge at <https://pubs.acs.org/doi/10.1021/acsomega.2c00804>.

Physicochemical characteristics of BEA materials (Figures S1–S3); <sup>31</sup>P MAS NMR spectra of bulk probe molecules (Figure S4); <sup>31</sup>P MAS NMR spectra of TBPO adsorbed on Al-BEA-25 recorded using a simple single-pulse sequence and a Hahn-echo pulse sequence (Figure S5); preliminary and quantitative assessment of the acidity of Al-BEA-25 zeolite by the adsorption procedures of R<sub>3</sub>PO using different techniques (Tables S1 and S2); T<sub>1</sub> relaxation time determination procedure and raw data (Figure S6); and <sup>1</sup>H MAS NMR spectra of studied BEA materials after removal of water at high temperatures (Figures S7) (PDF)

#### ■ AUTHOR INFORMATION

##### Corresponding Author

Irina I. Ivanova – Department of Chemistry, Lomonosov Moscow State University, 119991 Moscow, Russia; A.V. Topchiev Institute of Petrochemical Synthesis RAS, 119991 Moscow, Russia; [orcid.org/0000-0002-8742-2892](https://orcid.org/0000-0002-8742-2892); Email: [iiivanova@phys.chem.msu.ru](mailto:iiivanova@phys.chem.msu.ru)

##### Authors

Dmitry S. Zasukhin – Department of Chemistry, Lomonosov Moscow State University, 119991 Moscow, Russia;

[orcid.org/0000-0003-2110-0492](https://orcid.org/0000-0003-2110-0492)

Ivan A. Kasyanov – Department of Chemistry, Lomonosov Moscow State University, 119991 Moscow, Russia

Yury G. Kolyagin – Department of Chemistry, Lomonosov Moscow State University, 119991 Moscow, Russia; A.V.

Topchiev Institute of Petrochemical Synthesis RAS, 119991 Moscow, Russia; [orcid.org/0000-0001-8095-6923](https://orcid.org/0000-0001-8095-6923)

Anna I. Bulygina – Department of Chemistry, Lomonosov Moscow State University, 119991 Moscow, Russia

Karl C. Kharas – BASF Corporation, Iselin, New Jersey 08830, United States

Complete contact information is available at:

<https://pubs.acs.org/10.1021/acsomega.2c00804>

## Notes

The authors declare no competing financial interest.

## ACKNOWLEDGMENTS

This work was supported by the Russian Science Foundation (project no. 19-73-10160).

## REFERENCES

- (1) Auerbach, S. M.; Carrado, K. A.; Dutta, P. K. *Handbook of Zeolite Science and Technology*; CRC Press, 2003; p 1204
- (2) Derouane, E. G.; Vedin, J. C.; Pinto, R. R.; Borges, P. M.; Costa, L.; Lemos, M.A.N.D.A.; Ribeiro, F. R.; et al. The acidity of zeolites: concepts, measurements and relation to catalysis: a review on experimental and theoretical methods for the study of zeolite acidity. *Catal. Rev.* **2013**, *55*, 454–515.
- (3) Zheng, A.; Liu, S. B.; Deng, F.  $^{31}\text{P}$  NMR chemical shifts of phosphorus probes as reliable and practical acidity scales for solid and liquid catalysts. *Chem. Rev.* **2017**, *117*, 12475–12531.
- (4) Farneth, W. E.; Gorte, R. J. Methods for characterizing zeolite acidity. *Chem. Rev.* **1995**, *95*, 615–636.
- (5) Niwa, M.; Katada, N.; Sawa, M.; Murakami, Y. Temperature-programmed desorption of ammonia with readsorption based on the derived theoretical equation. *J. Phys. Chem. A* **1995**, *99*, 8812–8816.
- (6) Lercher, J. A.; Gründling, C.; Eder-Mirth, G. Infrared studies of the surface acidity of oxides and zeolites using adsorbed probe molecules. *Catal. Today* **1996**, *27*, 353–376.
- (7) Sarv, P.; Tuhern, T.; Lippmaa, E.; Keskinen, E.; Root, A. Mobility of the acidic proton in Brønsted sites of H-Y, H-mordenite, and H-ZSM-5 zeolites, studied by high-temperature  $^1\text{H}$  MAS NMR. *J. Phys. Chem. B* **1995**, *99*, 13763–13768.
- (8) Corma, A.; Fornés, V.; Forní, L.; Márquez, F.; Martínez-Triguero, J.; Moscotti, D. 2,6-Di-tert-butyl-pyridine as a probe molecule to measure external acidity of zeolites. *J. Catal.* **1998**, *179*, 451–458.
- (9) Buzzoni, R.; Bordiga, S.; Ricchiardi, G.; Lamberti, C.; Zecchina, A.; Bellussi, G. Interaction of pyridine with acidic (H-ZSM5, H- $\beta$ , H-MORD zeolites) and superacidic (H-Nafion membrane) systems: An IR investigation. *Langmuir* **1996**, *12*, 930–940.
- (10) Fărcașiu, D.; Leu, R.; Corma, A. Evaluation of accessible acid sites on solids by  $^{15}\text{N}$  NMR spectroscopy with di-tert-butylpyridine as base. *J. Phys. Chem. B* **2002**, *106*, 928–932.
- (11) Zheng, A.; Deng, F.; Liu, S. B. Acidity Characterization of Solid Acid Catalysts by Solid-State  $^{31}\text{P}$  NMR of Adsorbed Phosphorus-Containing Probe Molecules. *Annu. Rep. NMR Spectrosc.* **2014**, *81*, 47–108.
- (12) Zasukhin, D. S.; Kostyukov, I. A.; Kasyanov, I. A.; Kolyagin, Y. G.; Ivanova, I. I.  $^{31}\text{P}$  NMR Spectroscopy of Adsorbed Probe Molecules as a Tool for the Determination of the Acidity of Molecular Sieve Catalysts (A Review). *Pet. Chem.* **2021**, *61*, 875–894.
- (13) Lunsford, J. H.; Rothwell, W. P.; Shen, W. Acid sites in zeolite Y: a solid-state NMR and infrared study using trimethylphosphine as a probe molecule. *J. Am. Chem. Soc.* **1985**, *107*, 1540–1547.
- (14) Baltusis, L.; Frye, J. S.; Maciel, G. E. Phosphorus 31 NMR study of trialkylphosphine probes adsorbed on silica-alumina. *J. Am. Chem. Soc.* **1987**, *109*, 40–46.
- (15) Hu, B.; Gay, I. D.  $^{31}\text{P}$  NMR investigation of surface acidity using adsorbed tricyclohexylphosphine as a probe. *Langmuir* **1995**, *11*, 3845–3847.
- (16) Kao, H. M.; Yu, C. Y.; Yeh, M. C. Detection of the inhomogeneity of Brønsted acidity in H-mordenite and H- $\beta$  zeolites: a comparative NMR study using trimethylphosphine and trimethylphosphine oxide as  $^{31}\text{P}$  NMR probes. *Microporous Mesoporous Mater.* **2002**, *53*, 1–12.
- (17) Rieg, C.; Li, Z.; Kurtz, A.; Schmidt, M.; Dittmann, D.; Benz, M.; Dyballa, M. A Method for the Selective Quantification of Brønsted Acid Sites on External Surfaces and in Mesopores of Hierarchical Zeolites. *J. Phys. Chem. C* **2021**, *125*, 515–525.
- (18) Zhang, W.; Han, X.; Liu, X.; Bao, X. Characterization of the acid sites in dealuminated nanosized HZSM-5 zeolite with the probe molecule trimethylphosphine. *J. Mol. Catal. A: Chem.* **2003**, *194*, 107–113.
- (19) Zhuang, J.; Yan, Z.; Liu, X.; Liu, X.; Han, X.; Bao, X.; Mueller, U. NMR Study on the Acidity of TS-1 Zeolite. *Catal. Lett.* **2002**, *83*, 87–91.
- (20) Hu, B.; Gay, I. D. Probing surface acidity by  $^{31}\text{P}$  nuclear magnetic resonance spectroscopy of arylphosphines. *Langmuir* **1999**, *15*, 477–481.
- (21) Zalewski, D. J.; Chu, P. J.; Tutunjian, P. N.; Lunsford, J. H. The oxidation of trimethylphosphine in zeolite Y: a solid-state NMR study. *Langmuir* **1989**, *5*, 1026–1030.
- (22) Zheng, A.; Huang, S. J.; Chen, W. H.; Wu, P. H.; Zhang, H.; Lee, H. K.; De Menorval, L. C.; Deng, F.; Liu, S. B.  $^{31}\text{P}$  Chemical shift of adsorbed trialkylphosphine oxides for acidity characterization of solid acids catalysts. *J. Phys. Chem. A* **2008**, *112*, 7349–7356.
- (23) Osegovic, J. P.; Drago, R. S. Measurement of the global acidity of solid acids by  $^{31}\text{P}$  MAS NMR of chemisorbed triethylphosphine oxide. *J. Phys. Chem. B* **2000**, *104*, 147–154.
- (24) Zhao, Q.; Chen, W. H.; Huang, S. J.; Wu, Y. C.; Lee, H. K.; Liu, S. B. Discernment and quantification of internal and external acid sites on zeolites. *J. Phys. Chem. B* **2002**, *106*, 4462–4469.
- (25) Lewis, J. D.; Ha, M.; Luo, H.; Faucher, A.; Michaelis, V. K.; Román-Leshkov, Y. Distinguishing Active Site Identity in Sn-Beta Zeolites Using  $^{31}\text{P}$  MAS NMR of Adsorbed Trimethylphosphine Oxide. *ACS Catal.* **2018**, *8*, 3076–3086.
- (26) Freitas, C.; Barrow, N.; Zholobenko, V. Accessibility and Location of Acid Sites in Zeolites as Probed by Fourier Transform Infrared Spectroscopy and Magic Angle Spinning Nuclear Magnetic Resonance. *Johnson Matthey Technol. Rev.* **2018**, *62*, 279–290.
- (27) Rakiewicz, E. F.; Peters, A. W.; Wormsbecher, R. F.; Sutovich, K. J.; Mueller, K. T. Characterization of Acid Sites in Zeolitic and Other Inorganic Systems Using Solid-State  $^{31}\text{P}$  NMR of the Probe Molecule Trimethylphosphine Oxide. *J. Phys. Chem. B* **1998**, *102*, 2890–2896.
- (28) Lakiss, L.; Vicente, A.; Gilson, J.-P.; Valtchev, V.; Mintova, S.; Vimont, A.; Bedard, R.; Abdo, S.; Bricker, J. Probing the Brønsted Acidity of the External Surface of Faujasite-Type Zeolites. *ChemPhysChem* **2020**, *21*, 1873–1881.
- (29) Wolf, P.; Valla, M.; Nunez-Zarur, F.; Comas-Vives, A.; Rossini, A. J.; Firth, C.; Kallas, H.; Lesage, A.; Emsley, L.; Coperet, C.; Hermans, I. Correlating synthetic methods, morphology, atomic-level structure, and catalytic activity of Sn- $\beta$  catalysts. *ACS Catal.* **2016**, *6*, 4047–4063.
- (30) Kim, B.; Kim, C.; Ahn, D.; Moon, T.; Ahn, J.; Park, Y.; Park, B. Nanostructural effect of  $\text{AlPO}_4$ -nanoparticle coating on the cycle-life performance in  $\text{LiCoO}_2$  thin films. *Electrochem. Solid-state Lett.* **2007**, *10*, A32–A35.
- (31) Knyazeva, E. E.; Konnov, S. V.; Shutkina, O. V.; Dobryakova, I. V.; Ponomareva, O. A.; Ivanova, I. I. Microporous crystalline silicoaluminophosphates: Effect of synthesis conditions on the physicochemical and catalytic properties in the reaction of methanol to  $\text{C}_2$ - $\text{C}_4$  olefins conversion. *Pet. Chem.* **2014**, *54*, 288–295.
- (32) Tamura, M.; Shimizu, K.; Satsuma, A. Comprehensive IR study on acid/base properties of metal oxides. *Appl. Catal., A* **2012**, *433–434*, 135–145.
- (33) Thakur, R. S.; Kurur, N. D.; Madhu, P. K. Swept-frequency two-pulse phase modulation for heteronuclear dipolar decoupling in solid-state NMR. *Chem. Phys. Lett.* **2006**, *426*, 459–463.

- (34) Markley, J. L.; Horsley, W. J.; Klein, M. P. Spin–lattice relaxation measurements in slowly relaxing complex spectra. *J. Chem. Phys.* **1971**, *55*, 3604–3605.
- (35) Dai, W.; Lei, Q.; Wu, G.; Guan, N.; Hunger, M.; Li, L. Spectroscopic Signature of Lewis Acidic Framework and Extraframework Sn Sites in Beta Zeolites. *ACS Catal.* **2020**, *10*, 14135–14146.
- (36) Zheng, A.; Huang, S. J.; Liu, S. B.; Deng, F. Acid properties of solid acid catalysts characterized by solid-state  $^{31}\text{P}$  NMR of adsorbed phosphorous probe molecules. *Phys. Chem. Chem. Phys.* **2011**, *13*, 14889–14901.
- (37) Zhao, R.; Zhao, Z.; Li, S.; Zhang, W. Insights into the Correlation of Aluminum Distribution and Brønsted Acidity in H-Beta Zeolites from Solid-State NMR Spectroscopy and DFT Calculations. *J. Phys. Chem. Lett.* **2017**, *8*, 2323–2327.
- (38) Wang, Y.; Xin, S.; Chu, Y.; Xu, J.; Qi, G.; Wang, Q.; Xia, Q.; Deng, F. Influence of Trimethylphosphine Oxide Loading on the Measurement of Zeolite Acidity by Solid-State NMR Spectroscopy. *J. Phys. Chem. C* **2021**, *125*, 9497–9506.
- (39) Obenaus, U.; Dyballa, M.; Lang, S.; Scheibe, M.; Hunger, M. Generation and properties of Brønsted acid sites in bifunctional Rh-, Ir-, Pd-, and Pt-containing zeolites Y investigated by solid-state NMR spectroscopy. *J. Phys. Chem. C* **2015**, *119*, 15254–15262.
- (40) Evilia, R. F. Quantitative NMR spectroscopy. *Anal. Lett.* **2001**, *34*, 2227–2236.
- (41) Ernst, R. R.; Bodenhausen, G.; Wokaun, A. *Principles of Nuclear Magnetic Resonance in One and Two Dimensions*; Clarendon Press: Oxford, 1987; p 610.
- (42) Wang, X.; Coleman, J.; Jia, X.; White, J. L. Quantitative Investigations of Acidity, and Transient Acidity, in Zeolites and Molecular Sieves. *J. Phys. Chem. B* **2002**, *106*, 4941–4946.
- (43) Gerardin, C.; Haouas, M.; Lorentz, C.; Taulelle, F. NMR quantification in hydrothermal in situ syntheses. *Magn. Reson. Chem.* **2000**, *38*, 429–435.
- (44) Appelt, S.; Siefert, M.; Liebisch, A.; Blümich, B. External high-quality-factor resonator tunes up nuclear magnetic resonance. *Nat. Phys.* **2015**, *11*, 767–771.
- (45) Trombetta, M.; Armaroli, T.; Alejandre, A. G.; Solis, J. R.; Busca, G. An FT-IR study of the internal and external surfaces of HZSM5 zeolite. *Appl. Catal., A* **2000**, *192*, 125–136.
- (46) Marques, J. P.; Gener, I.; Ayrault, P.; Bordado, J. C.; Lopes, J. M.; Ribeiro, F. R.; Guisnet, M. Infrared spectroscopic study of the acid properties of dealuminated BEA zeolites. *Microporous Mesoporous Mater.* **2003**, *60*, 251–262.
- (47) Zholobenko, V.; Freitas, C.; Jendrlin, M.; Bazin, P.; Travert, A.; Thibault-Starzyk, F. Probing the acid sites of zeolites with pyridine: Quantitative AGIR measurements of the molar absorption coefficients. *J. Catal.* **2020**, *385*, 52–60.
- (48) Cambor, M. A.; Corma, A.; Valencia, S. Synthesis in fluoride media and characterisation of aluminosilicate zeolite beta. *J. Mater. Chem.* **1998**, *8*, 2137–2145.